UNVEILING PARTICLE ACCELERATION & HIGH-ENERGY EMISSION PROCESSES IN HOT SPOTS

Giulia Migliori (DIFA/INAF-IRA, Bologna)
M.Orienti, L.Coccato, G.Brunetti, K.-H. Mack,
F.D’Ammando, M.A.Prieto, H.Nagai

Hot spots in Radio Galaxies

Jet termination regions in FRII radio galaxies: sites of strong particle acceleration & radiative dissipation; radio to X-ray emission.

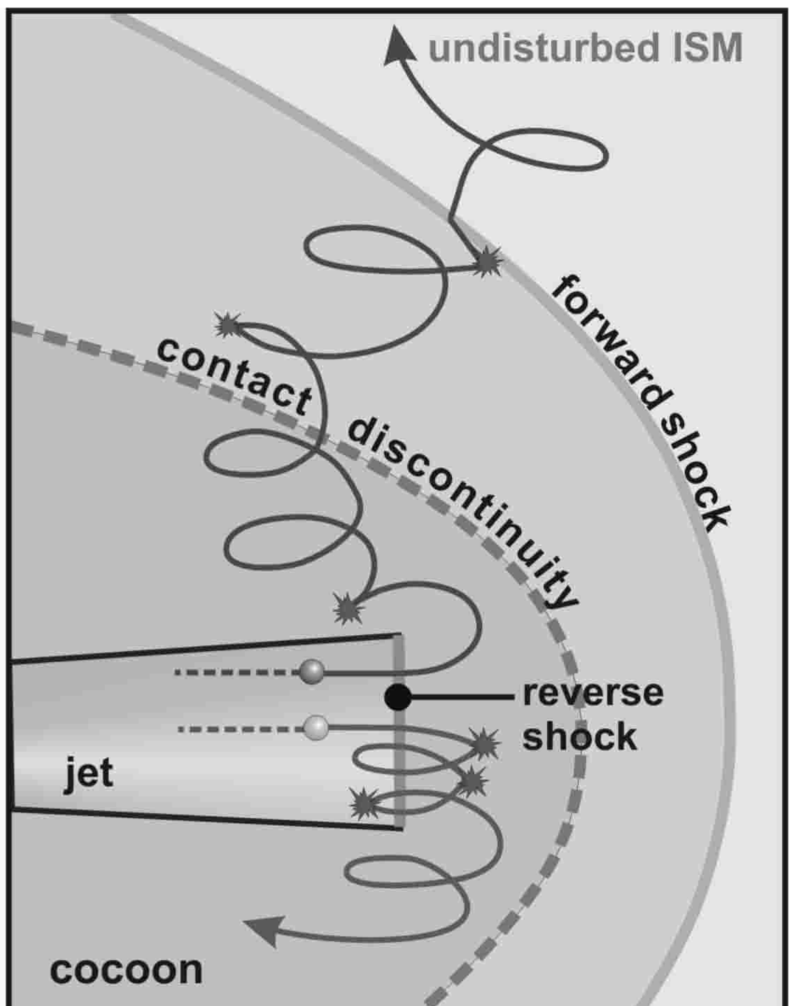

Heinz & Sunyaev`02

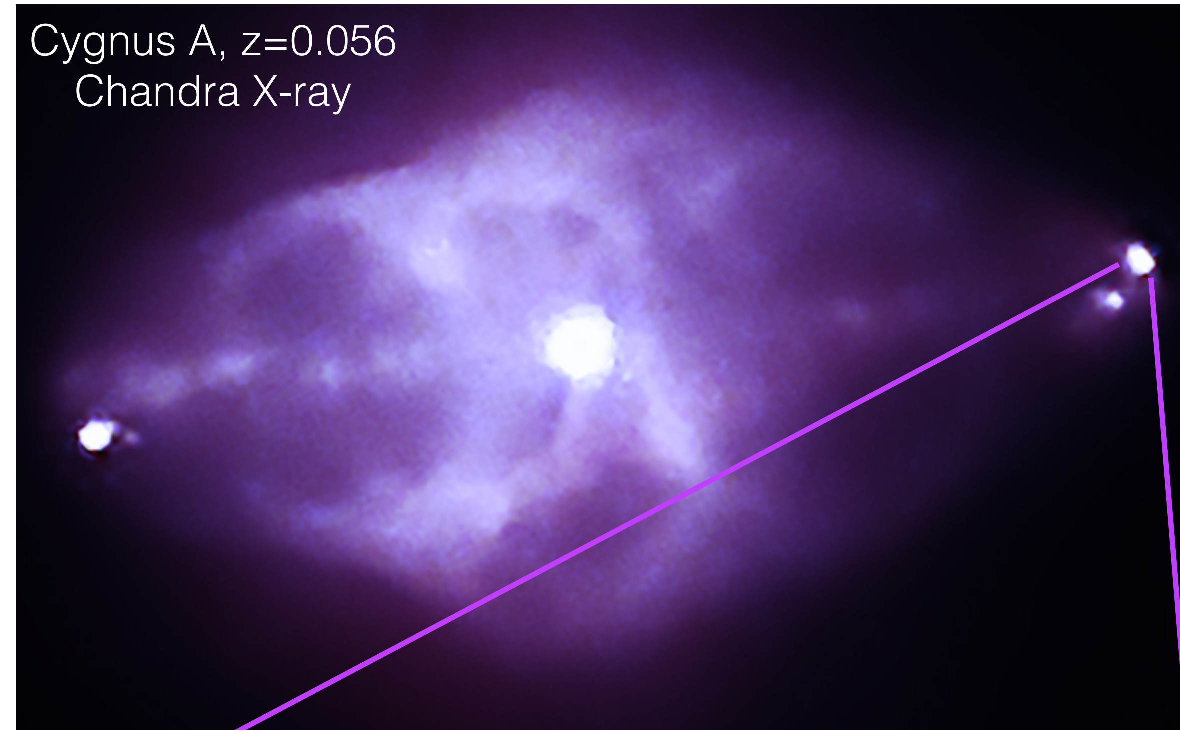

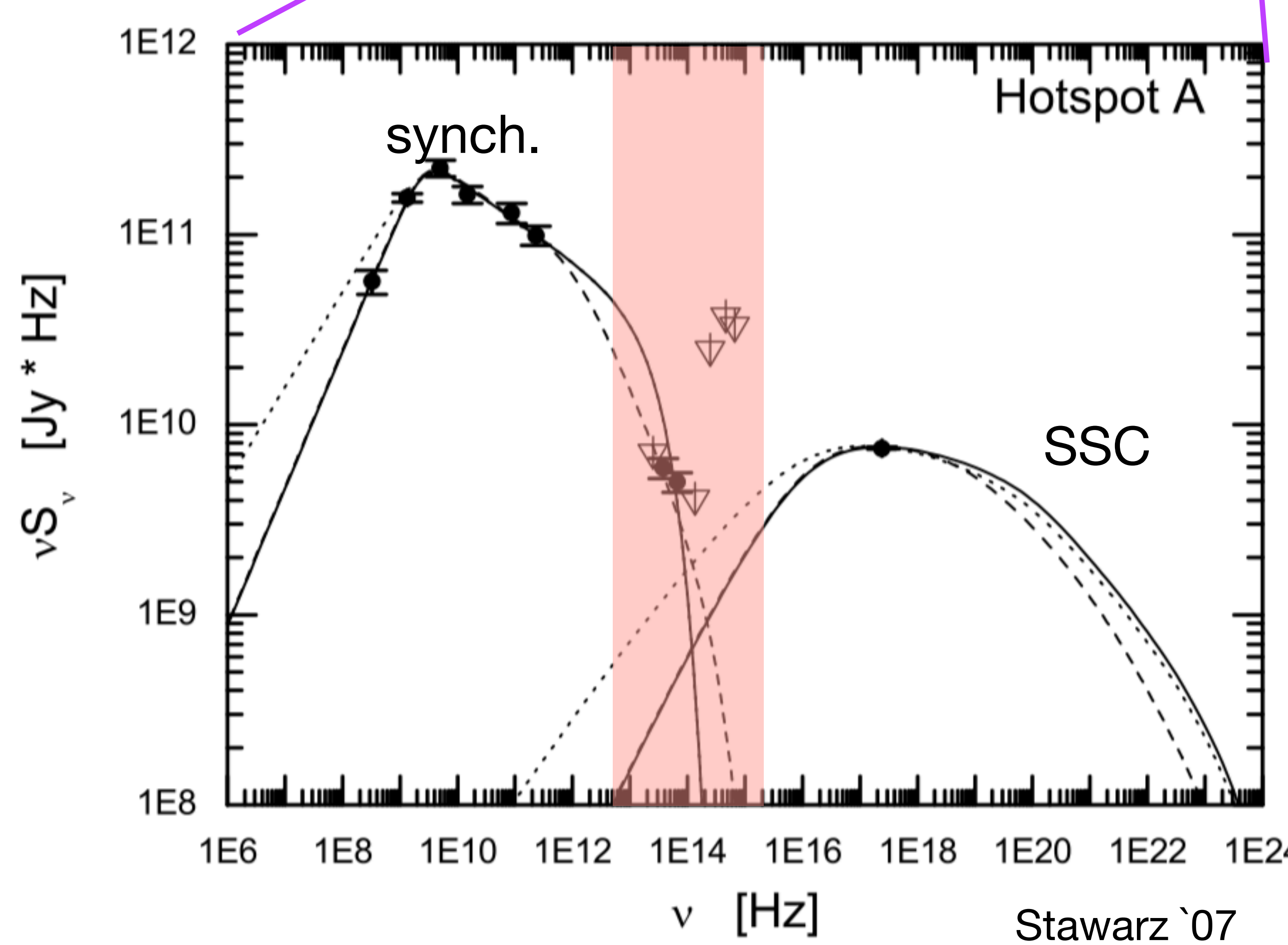

Stawarz `07

Low-power Hot spots: challenges to the standard picture

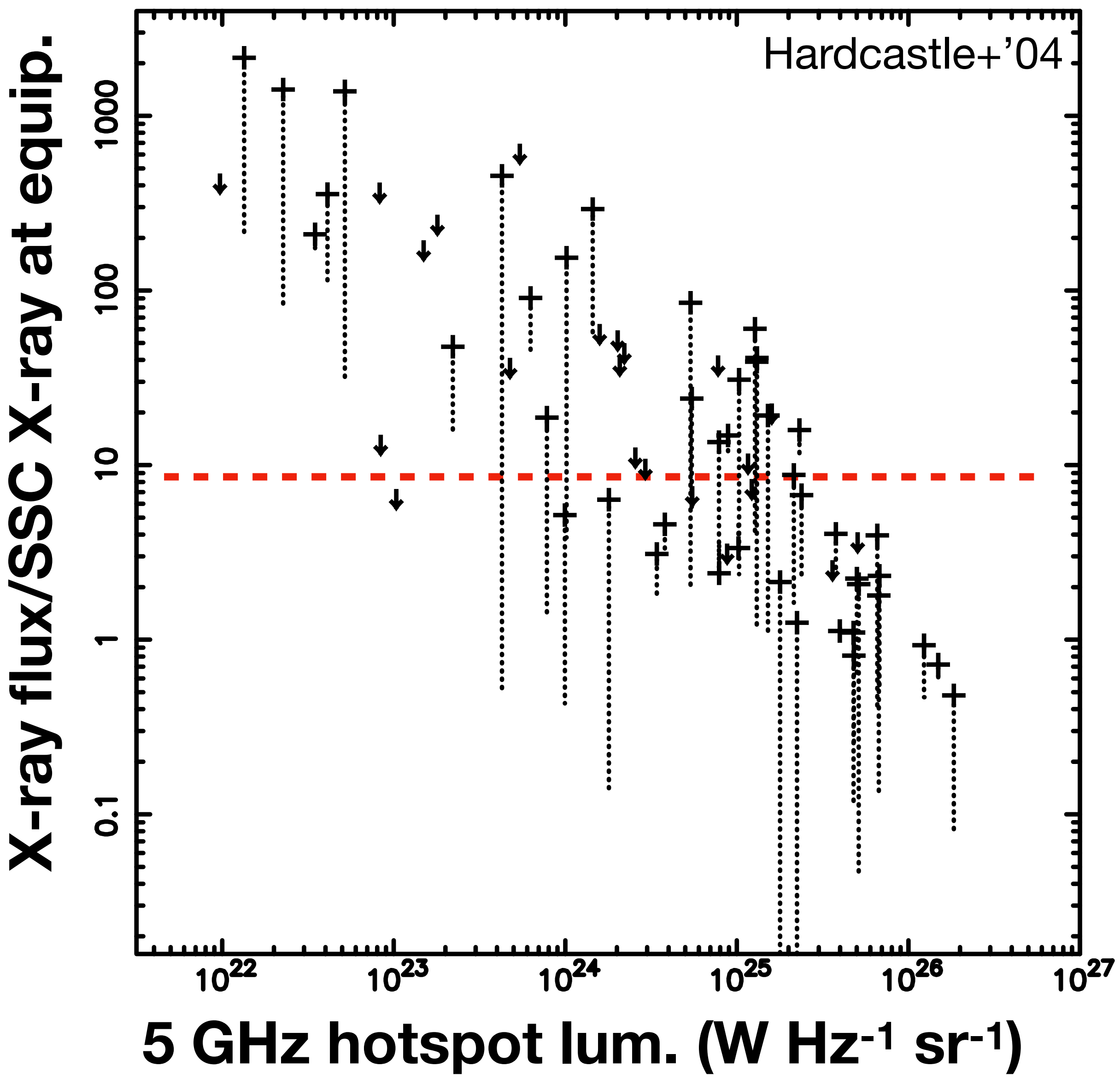

(I) low-luminous hot spots: SSC models require large departure from equipartition conditions ($U_e/U_B \gg 1$)

(II) offsets between radio and X-ray peaks;

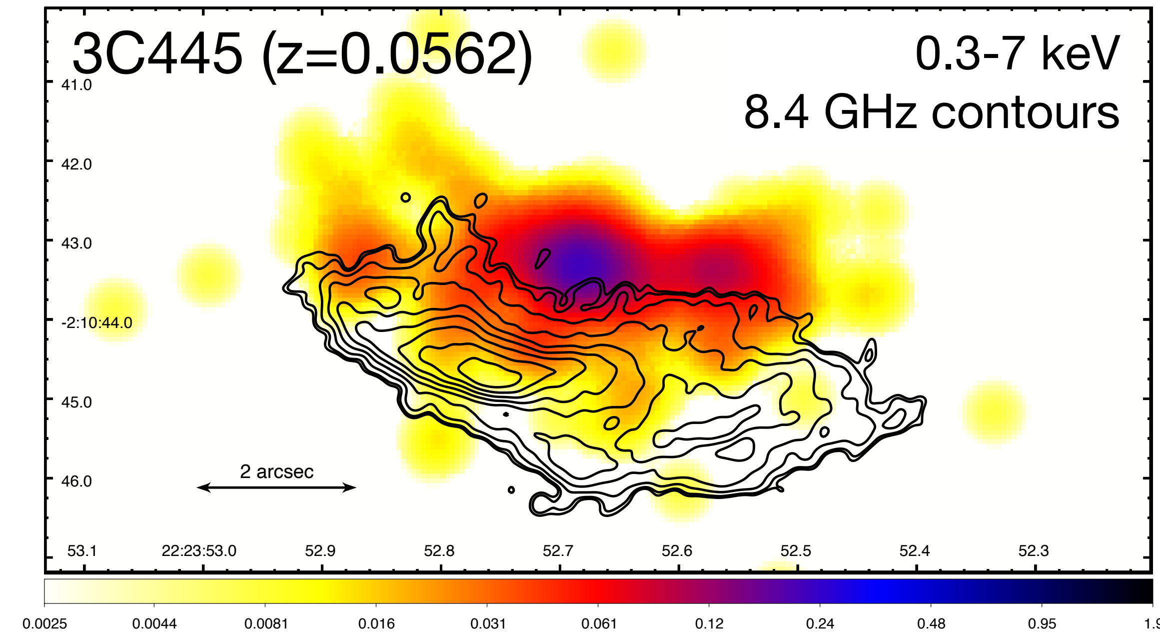

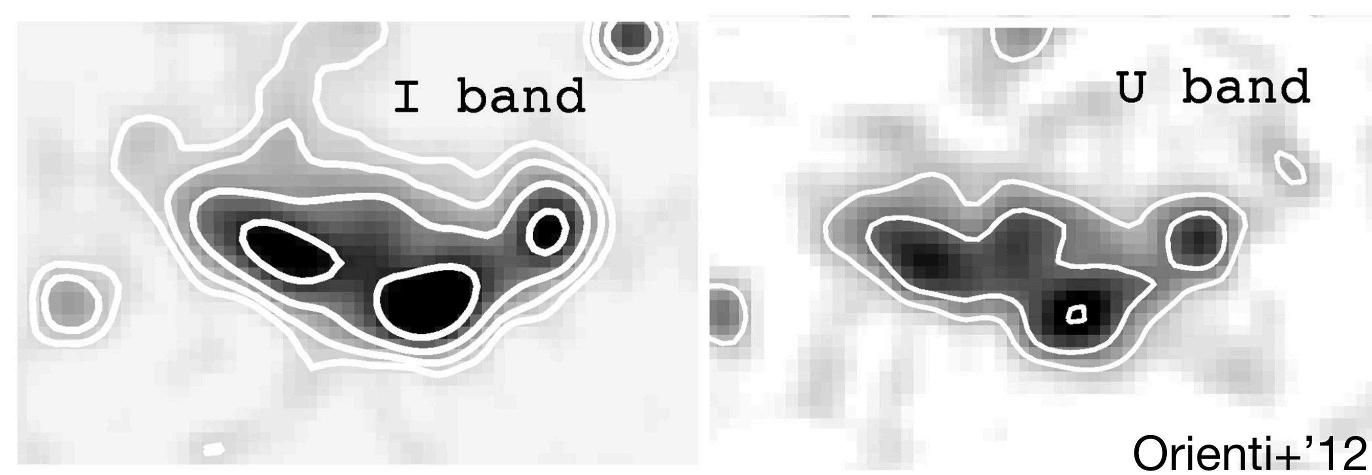

(III) detection of extended (kpc-scales) synchrotron optical emission

Low-power Hot spots: challenges to the standard picture

Open questions:

what's the origin of the X-ray emission?

only one site of particle acceleration?

(Meisenheimer+98,97, Prieto+'02, Hardcastle+04,07, Cheung+05, Mack+09, Perlman+'10,Werner+12, Orienti+12,17, Araudo+'16, Zhang+'18)

This work: study of a small sample of low-power hotspots of 3C radio galaxies selected from the NIR/optical study of Mack+'09

- **near-infrared & optical VLT data:** K (1.35×10^{14} Hz), H (1.87×10^{14} Hz), J (2.4×10^{14} Hz), R (4.29×10^{14} Hz), B (6.98×10^{14} Hz) bands => look for & constrain the extended optical component;
- **JVLA 22 GHz observations** (ang. res. 0.08"x0.07") => probe the hotspot structure & magnetic field at small (<kpc) scales;
- **SED modeling** => test of the X-ray radiative processes.

Migliori+'20: https://ui.adsabs.harvard.edu/abs/2020MNRAS.495.1593M/abstract
Orienti+'20:https://ui.adsabs.harvard.edu/abs/2020MNRAS.494.2244O/abstract

3C227 West

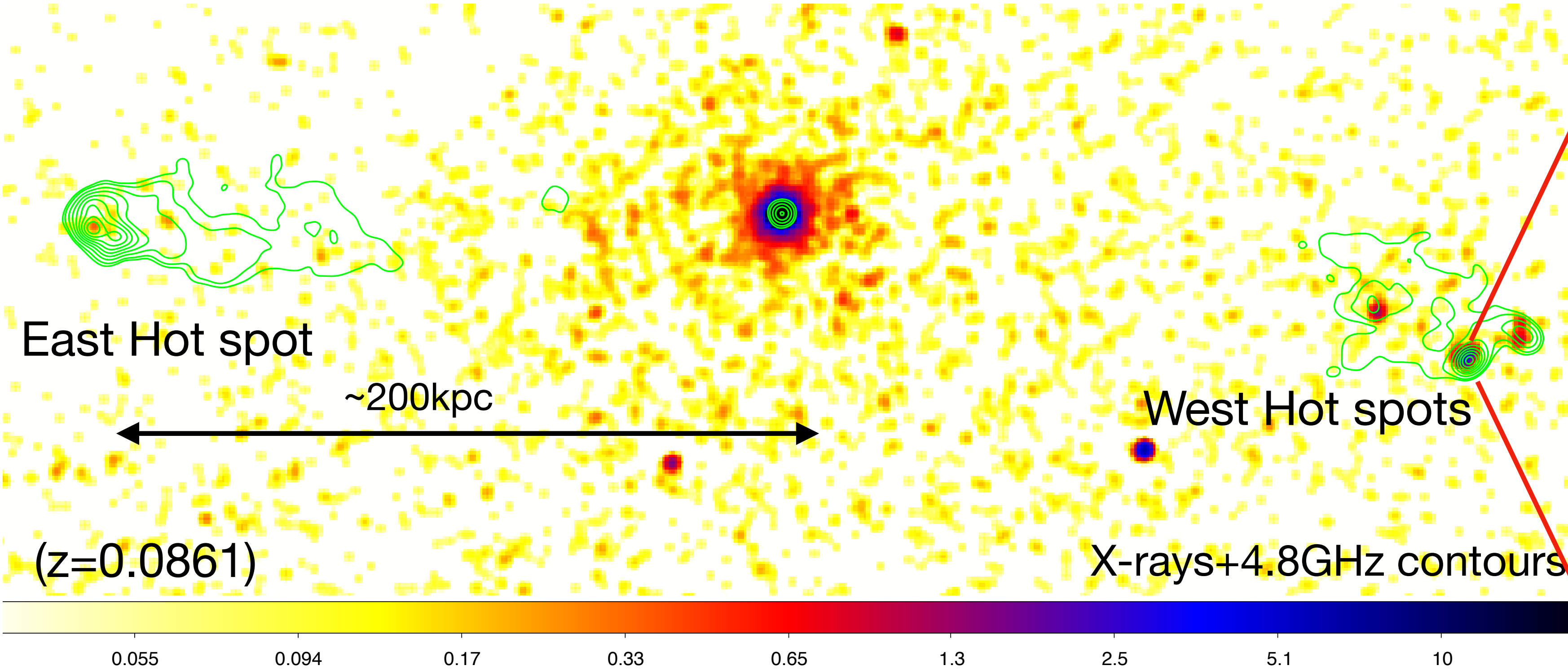

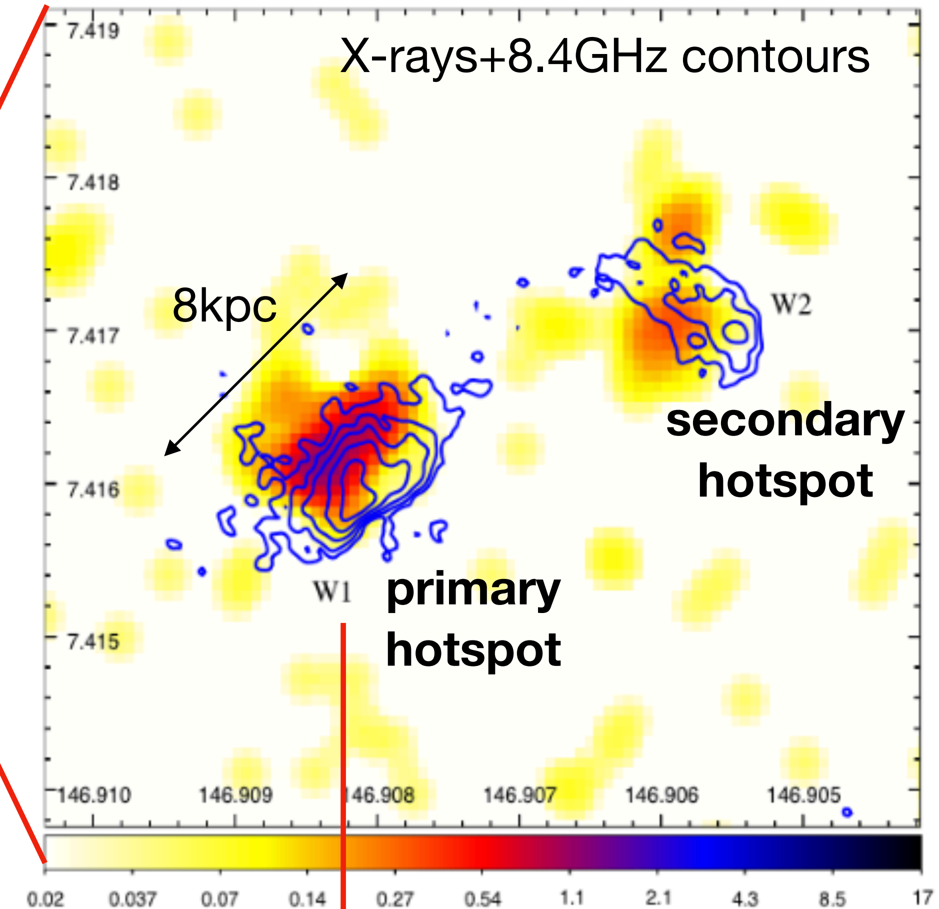

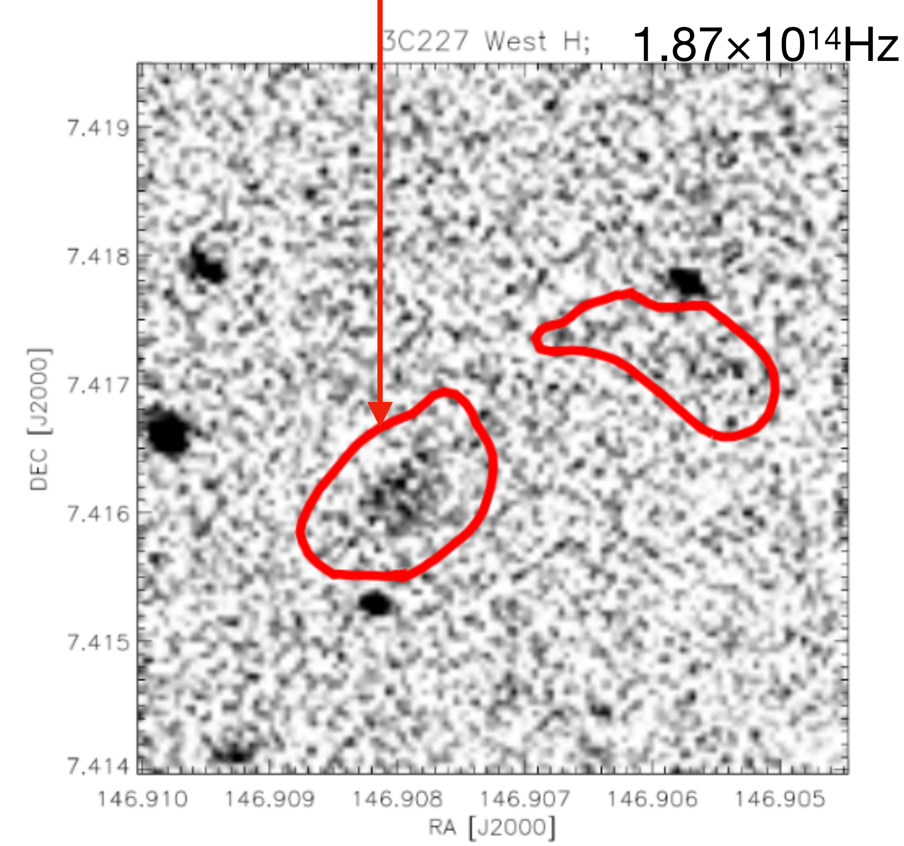

Radio vs. X-ray centroid offset:
0.8”±0.1”/1.3±0.2 kpc (Hardcastle+’07)

resolved NIR/optical emission co-spatial with the radio structure

3C227 West

JVLA observations @22 GHz (high. res. 0.08”x0.07”):
10% of the flux produced in
unresolved (<100 pc) regions with highly ordered magnetic field (≲60% fractional polarization)

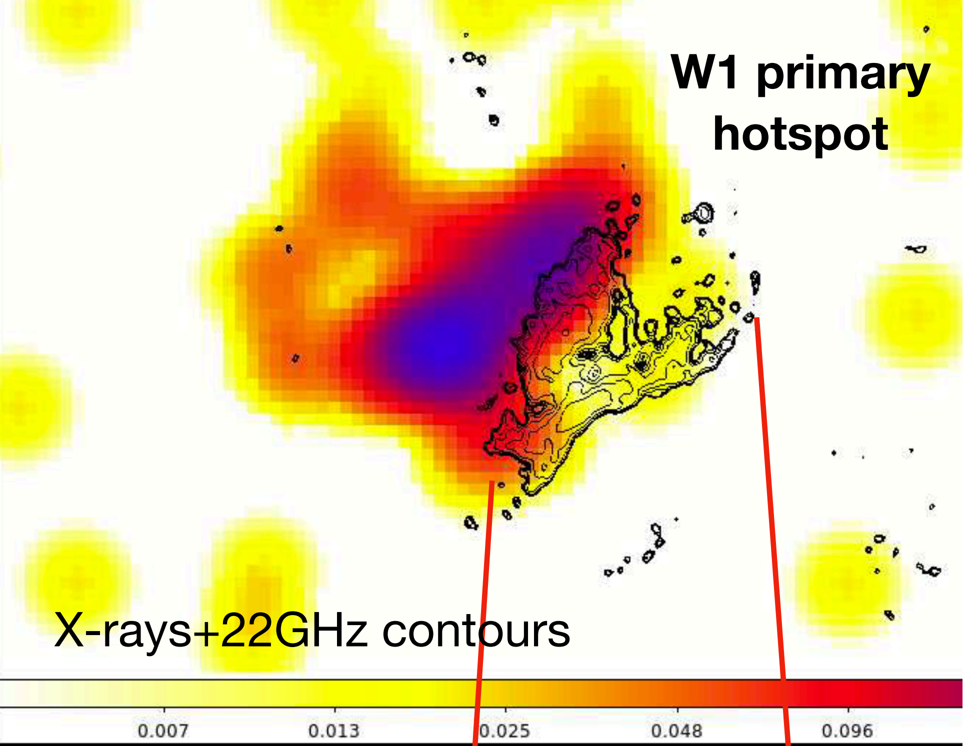

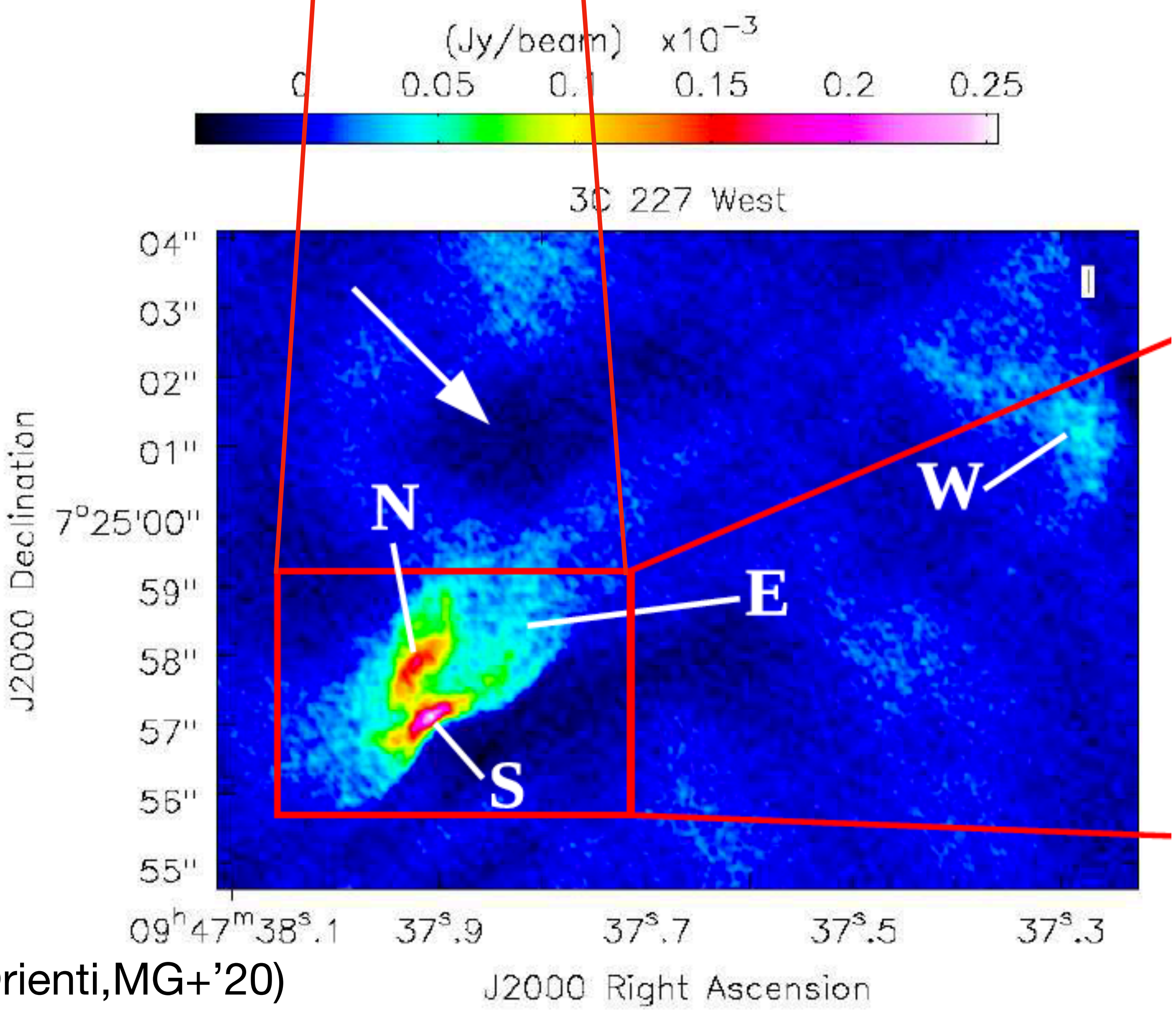

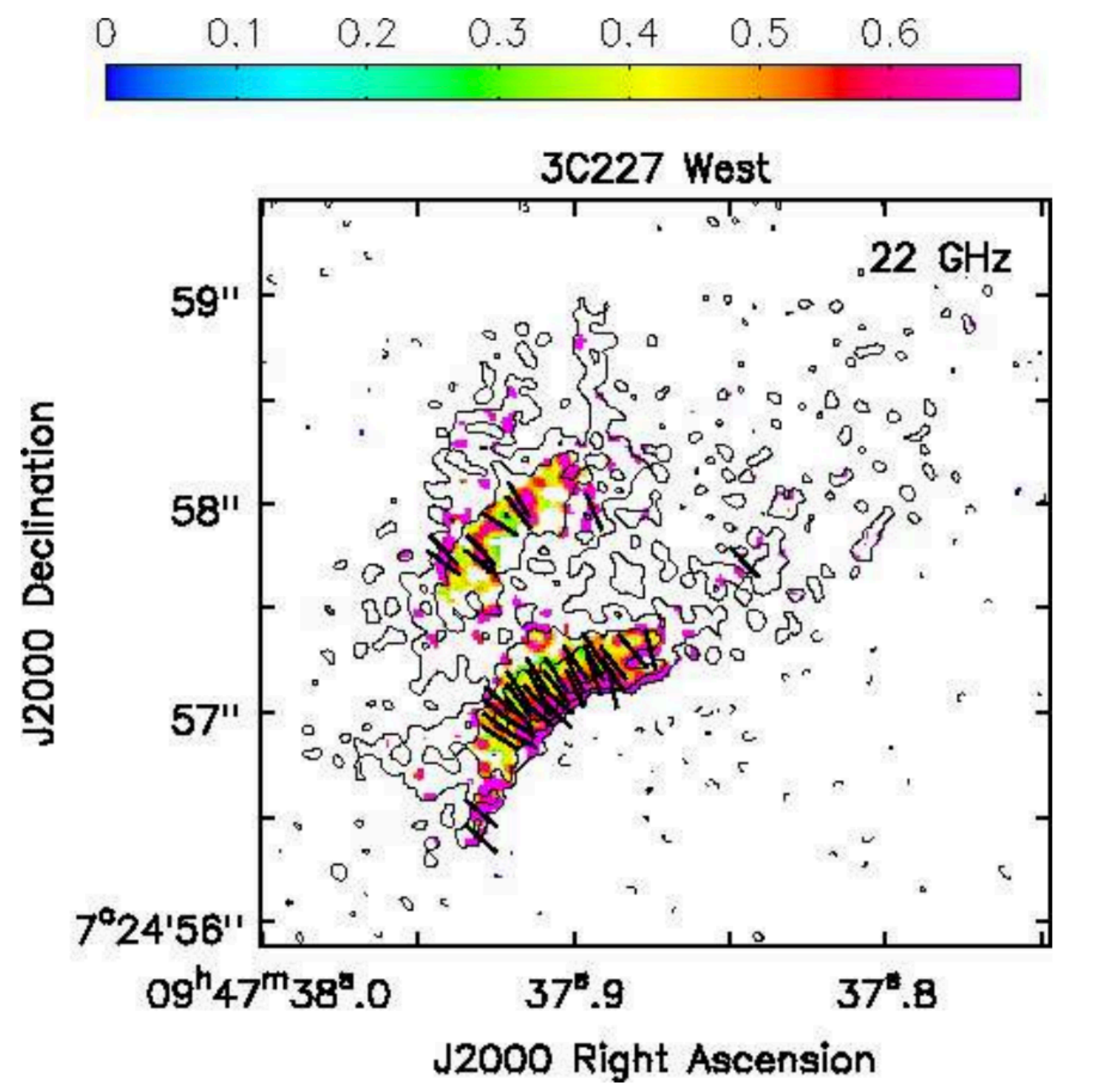

(Orienti,MG+’20)

Pictor A West Hot spot:

compact (16pc) radio clumps embedded in larger (~100pc) scale structure

+

indications of 10% **flux variability in X-rays** over 15 yrs timescale

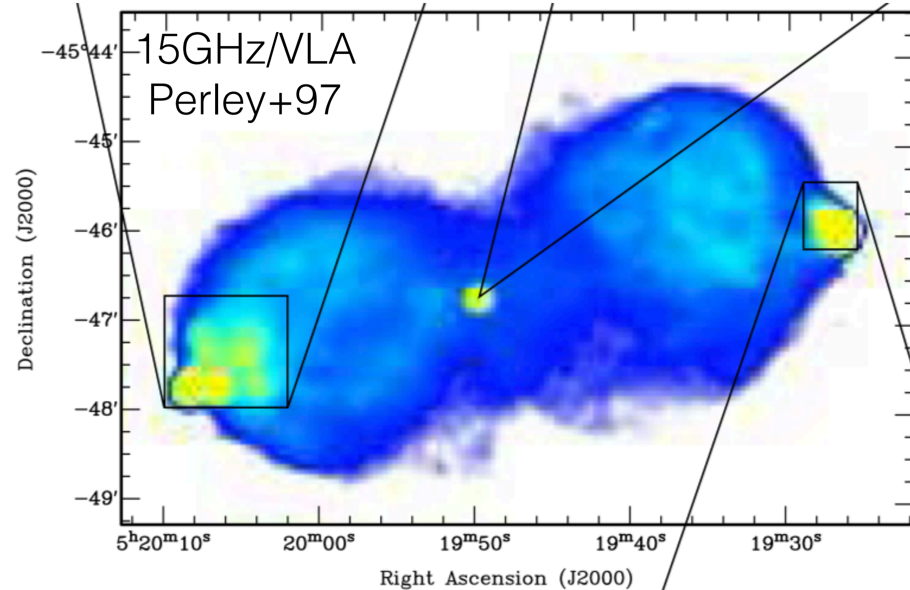

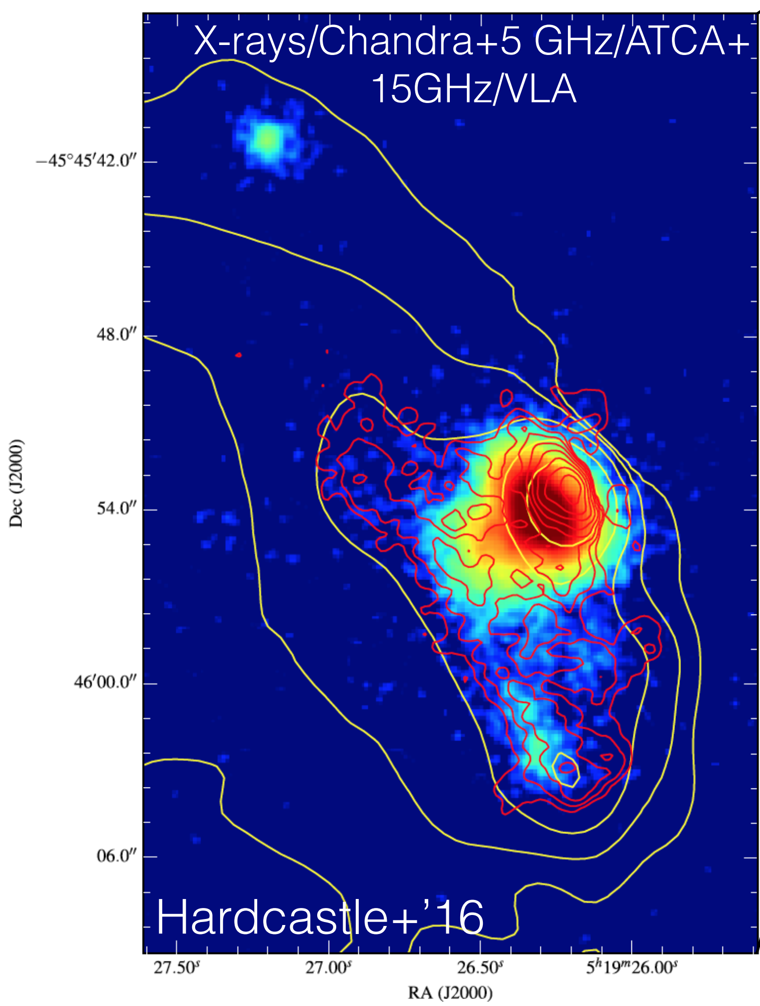

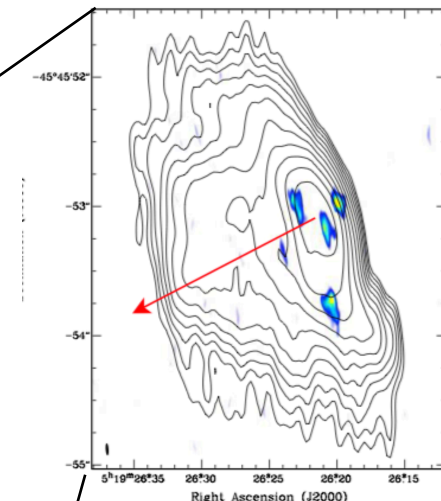

1.7GHz/VLBA
Tingay+'08

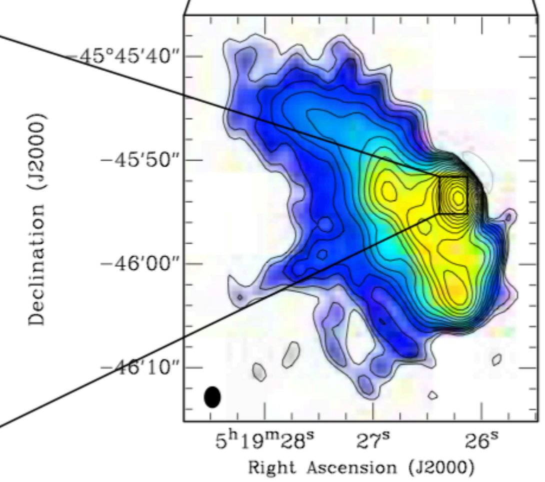

Tingay+'08

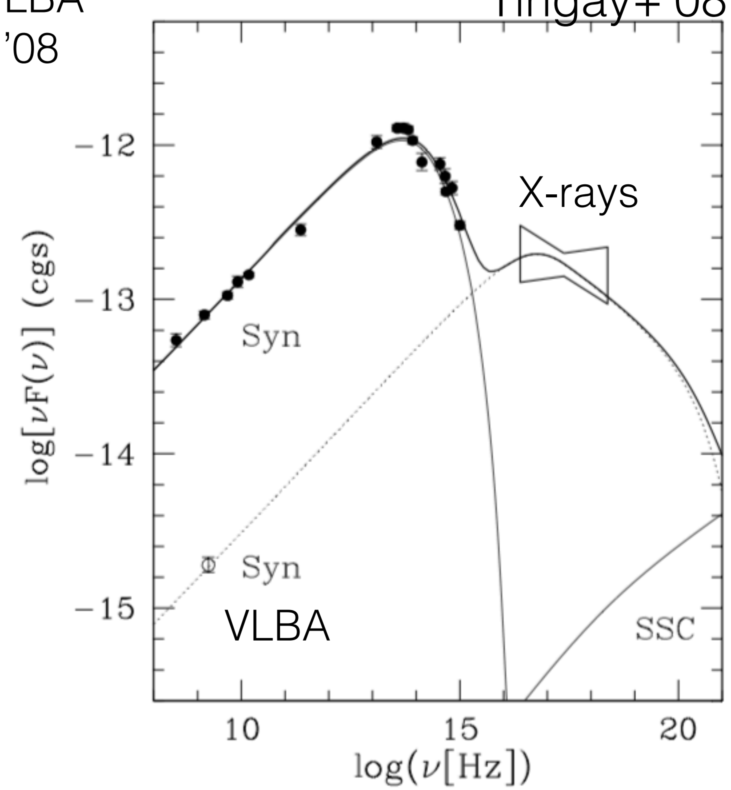

X-rays: **second synchrotron component** due to e⁻ accelerated by shocks in the compact clumps?

3C227 West: origin of the X-ray emission?

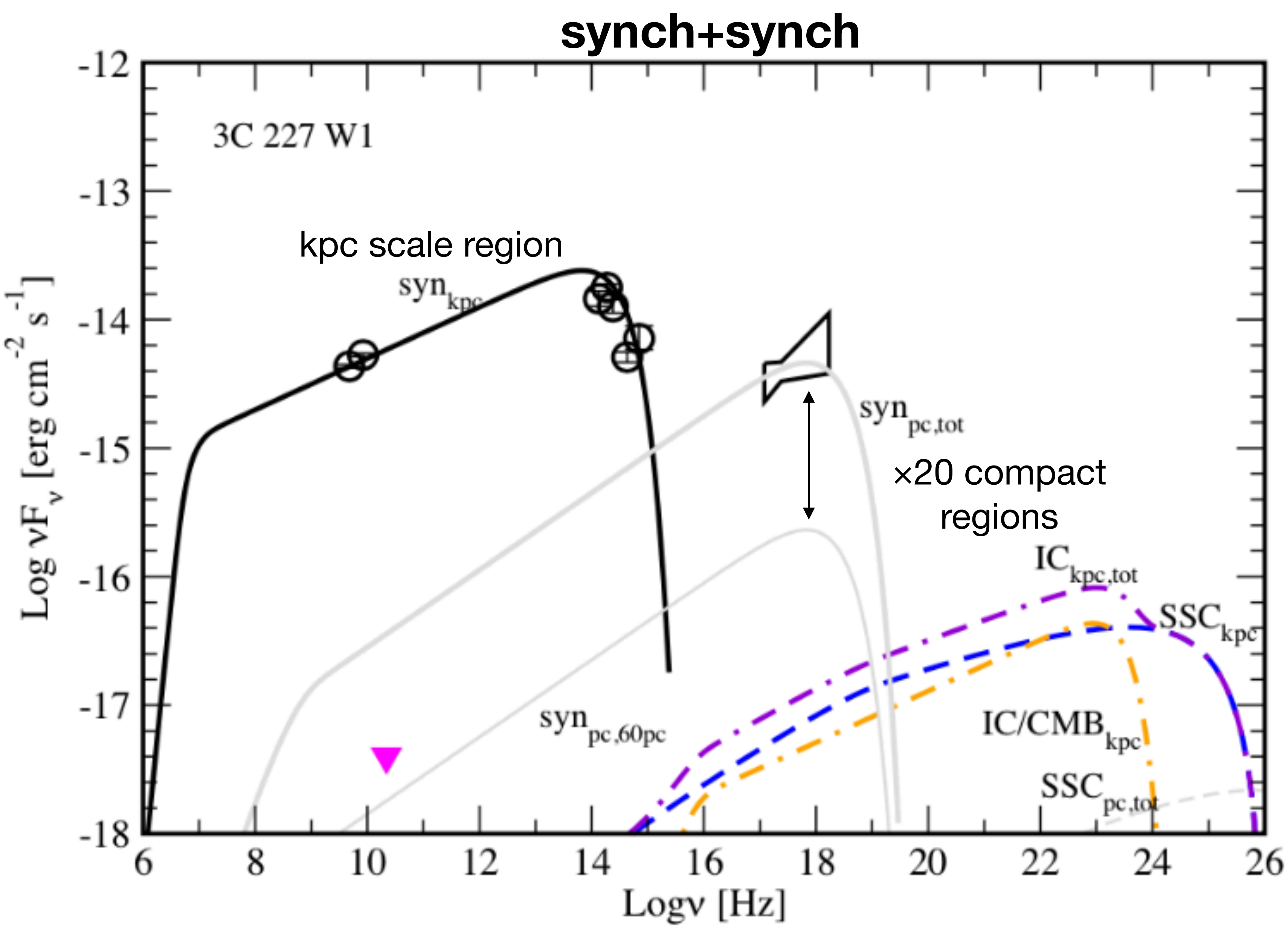

- the bulk of the radio to NIR/optical flux: synchrotron from the large scale (kpc) structure;
- X-rays: **synchrotron emission from clumps** with linear scales similar or smaller than the structures 'seen' at 22 GHz;
- the Lorentz factor of the **electrons giving the X-rays is γ_{max}~10^7-10^8** (assuming B_{eq}~70μG);
- possible scenario: X-rays trace the most recent acceleration sites while radio emission is the sum of multiple acceleration episodes

Conclusions & Future work

- Detection of highly polarised radio clumps in a small sample of low-power hotspots: how frequent are compact regions?

- monitoring over year-timescales can probe the sites where the most energetic particles are accelerated: multi-epoch X-ray observations of 3C445 S (in progress);

- Multi-band observations are key to unveil the complex acceleration and radiative mechanisms in the hot spots: detection of diffuse NIR/optical emission => role of turbulence?

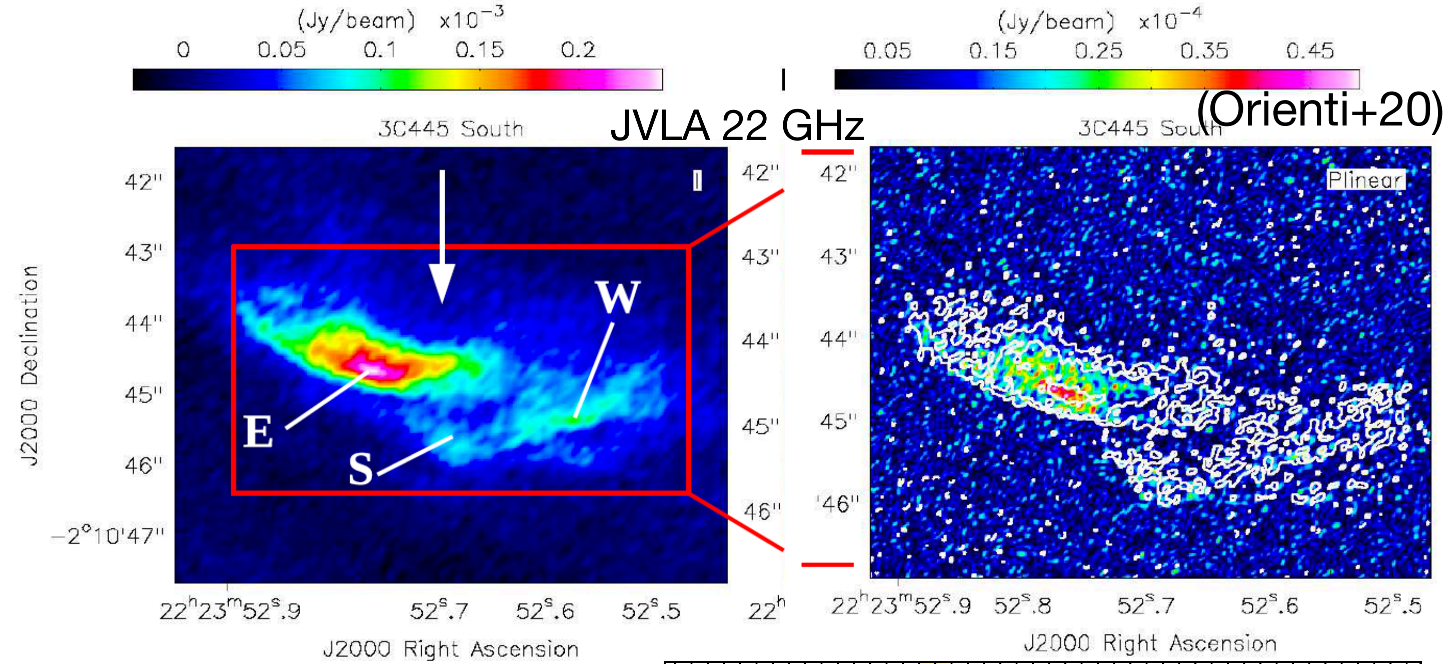

3C445 S

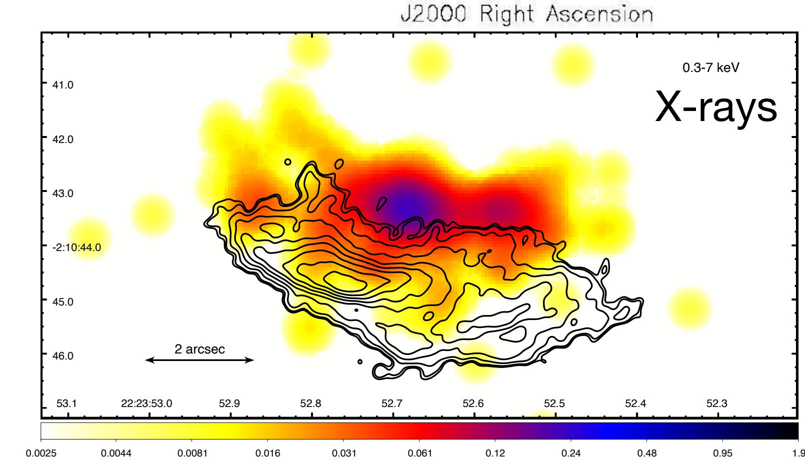

3C105 S

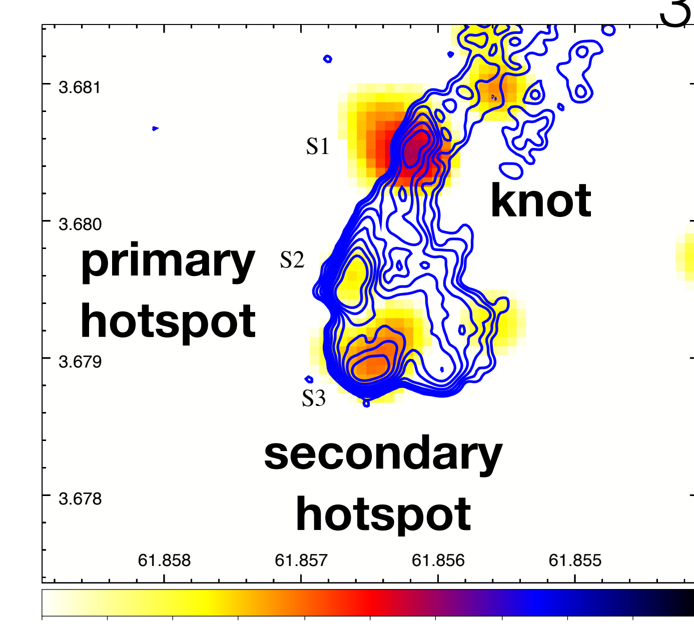

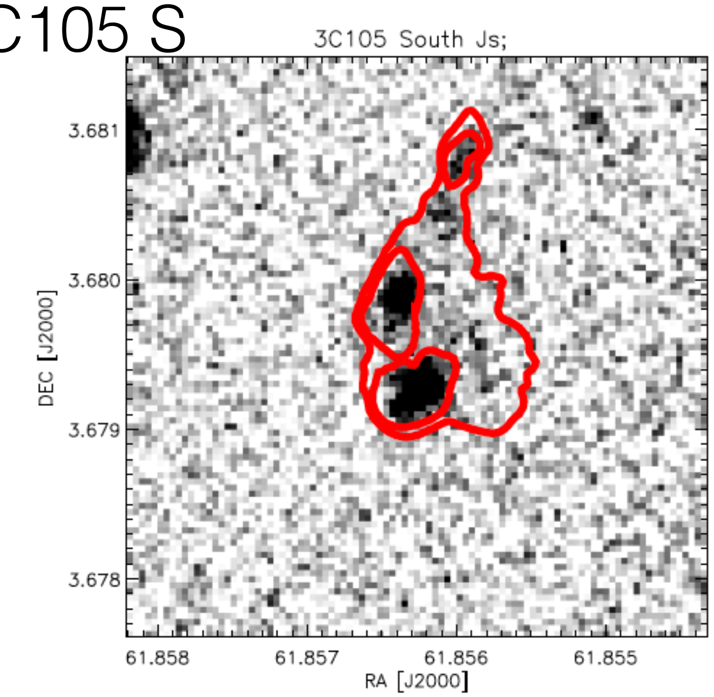

Conclusions & Future work

- macro to micro & micro to macro: simulations

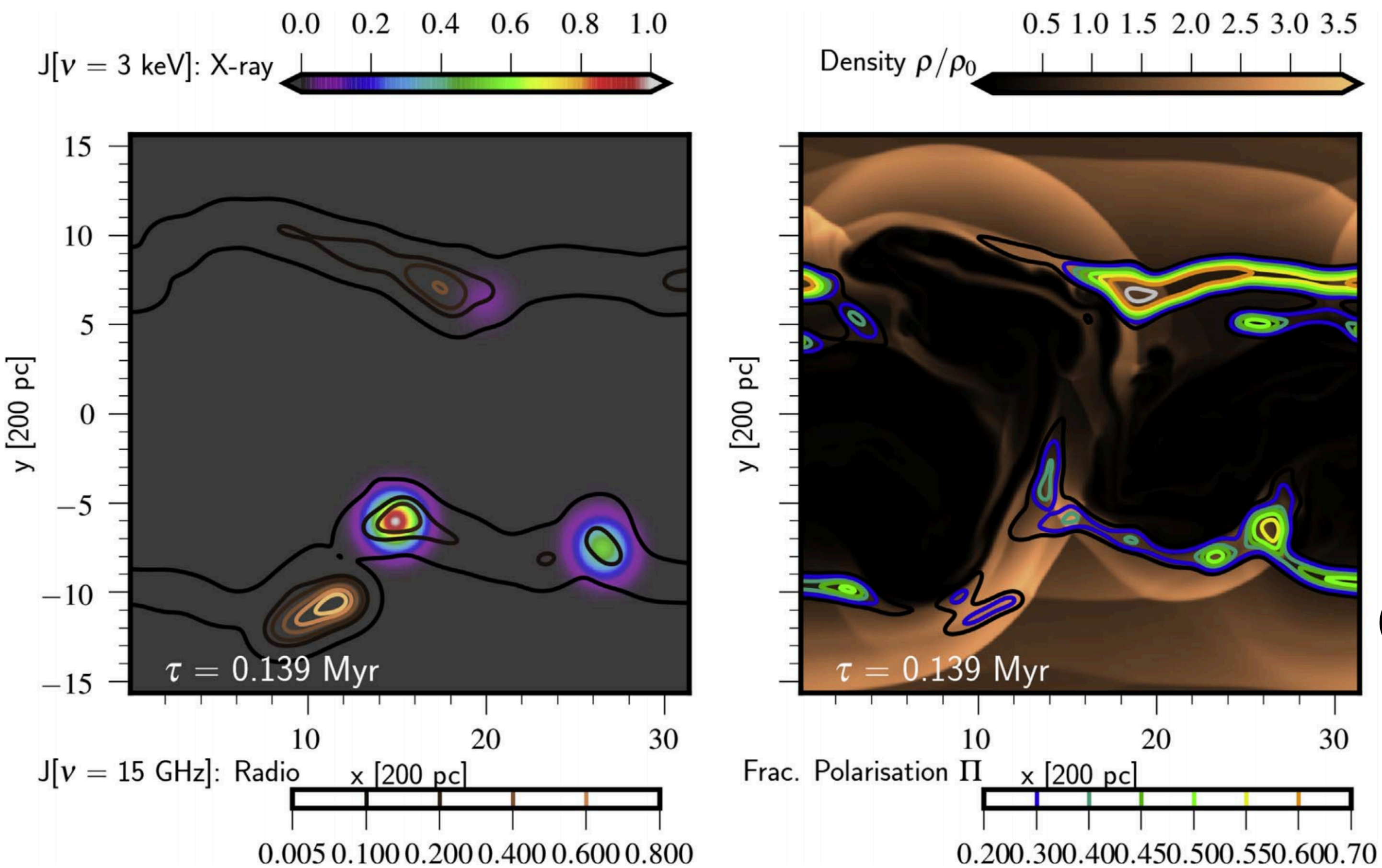

(Vaidya+18)

(Mukherjee+21)

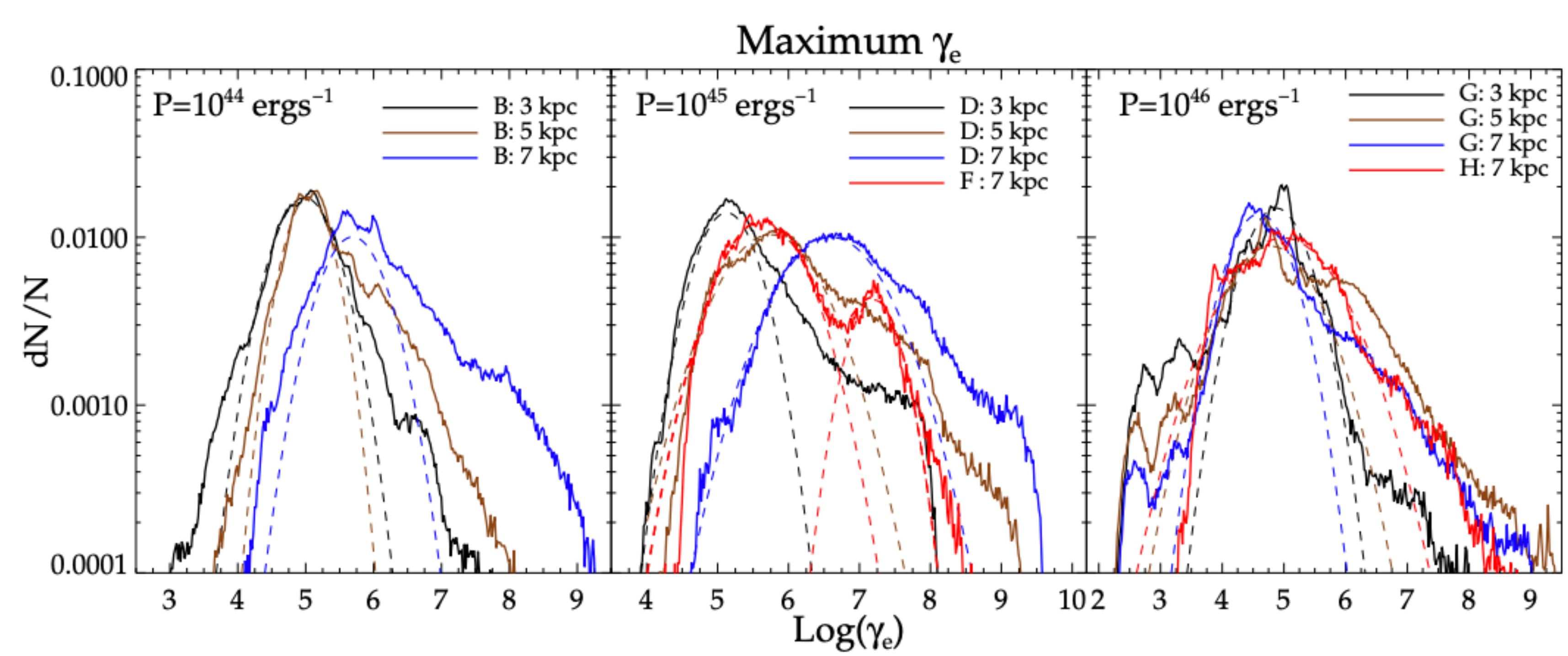

3C227 W1: origin of the X-ray emission?

synch+IC

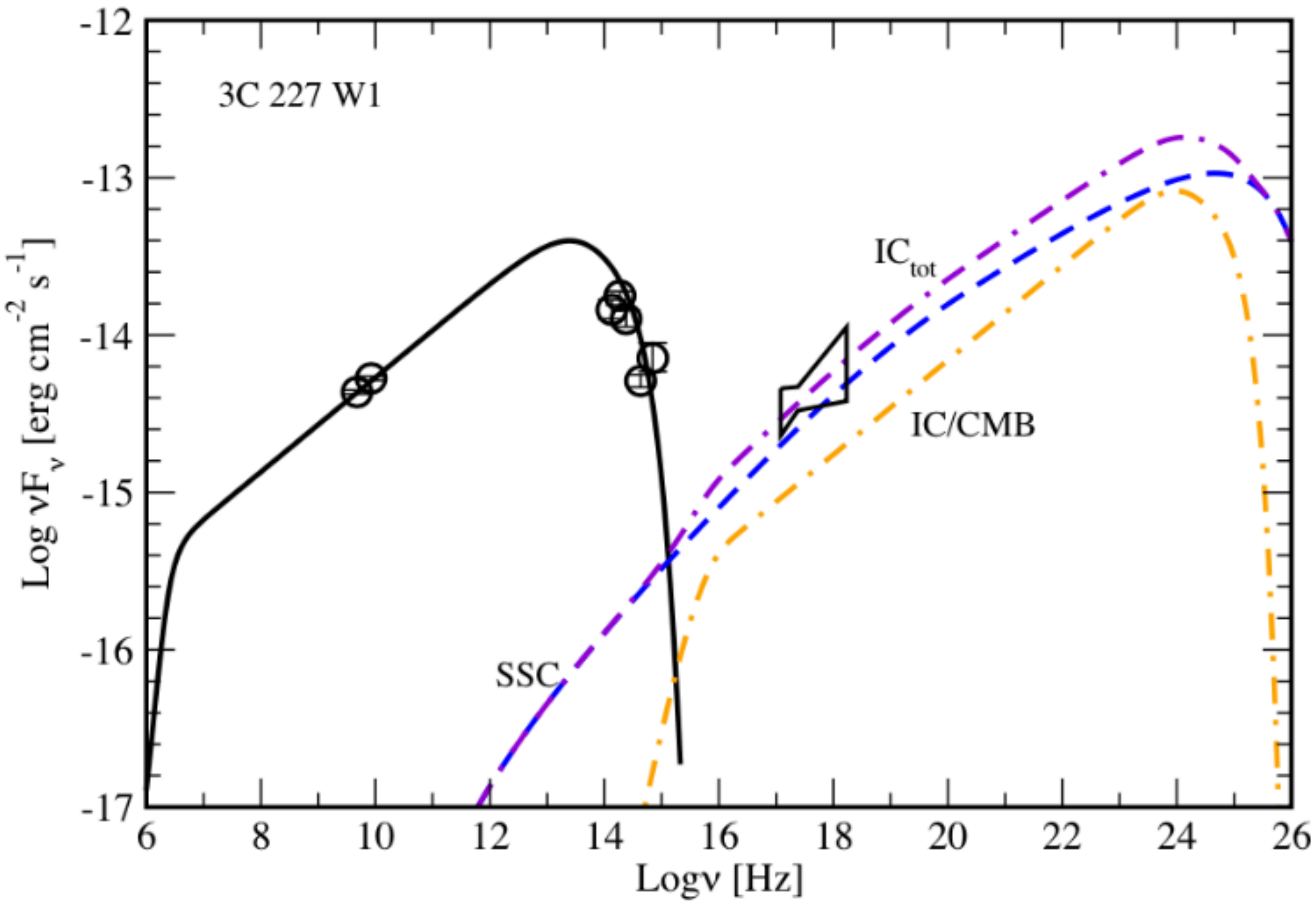

Migliori+20

- X-rays are produced via SSC + IC/CMB, but $U_B << U_e$ (B=2 μG, vs Beq~70 μG) and large jet powers (>10^{45} erg/s);
- assuming Doppler boosting (Γ_{bulk}~4 and θ~20, and U_B~U_e), X-rays from IC/CMB. However: 1- the jet power is ~10^{46} erg/s; 2- large-scale structure symmetry disfavors small θ; 3- unexplained radio-X-ray offset (see also Georganopoulos & Kazanas'04)?

Diffuse NIR-optical emission: 3C105

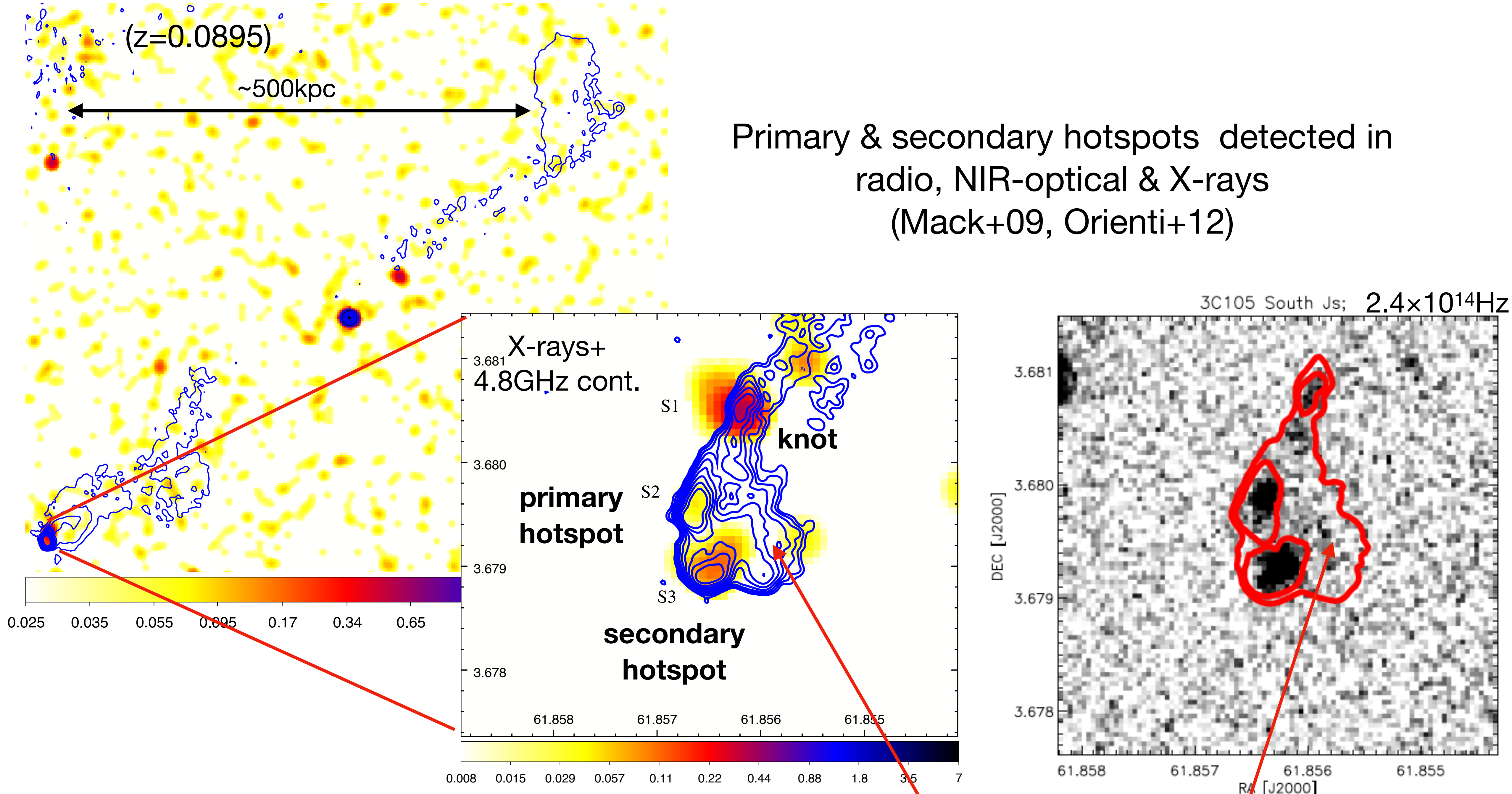

Primary & secondary hotspots detected in radio, NIR-optical & X-rays (Mack+09, Orienti+12)

<u>Diffuse</u> radio+NIR-optical emission
no X-rays

3C 105 South: diffuse NIR-optical emission

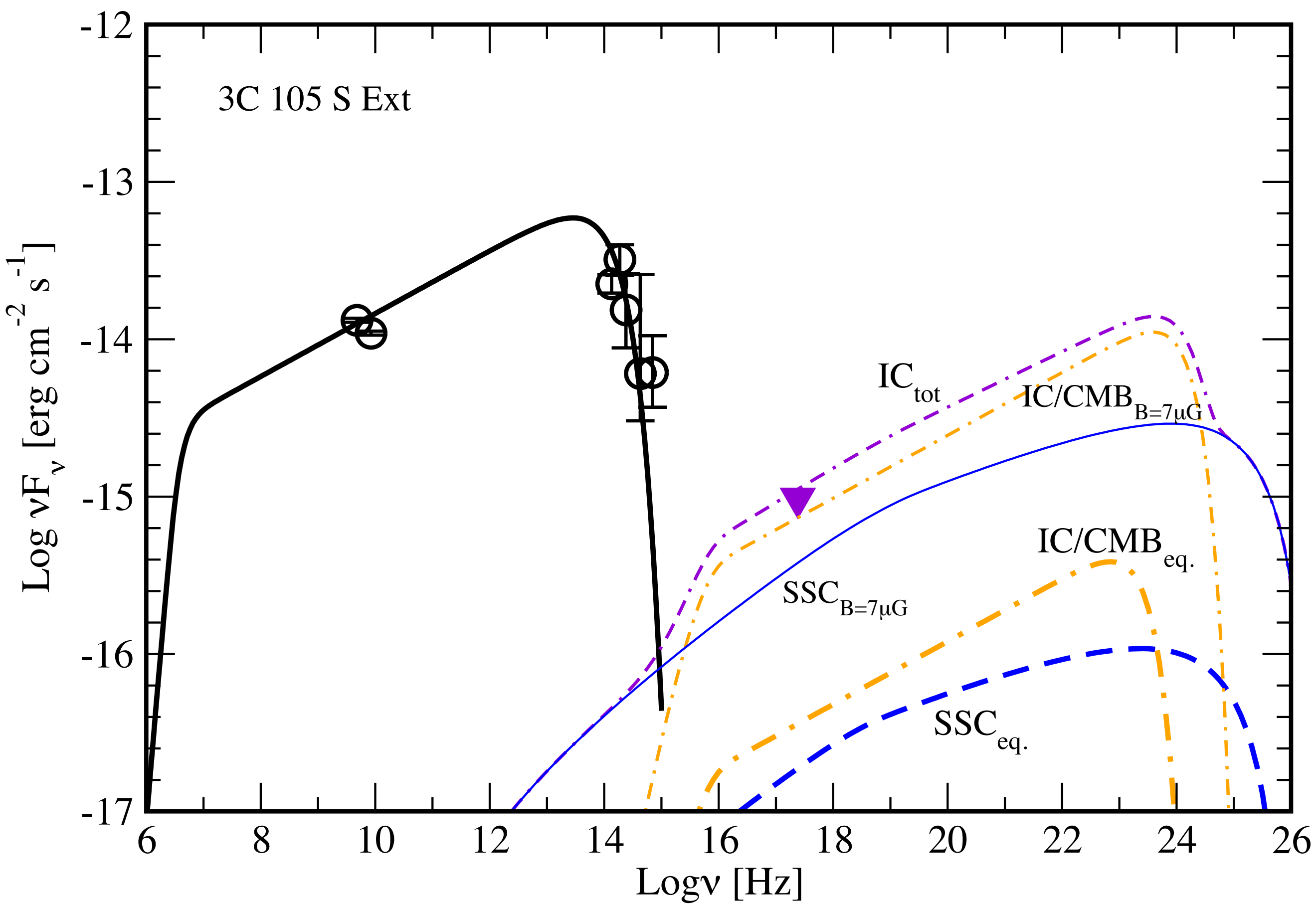

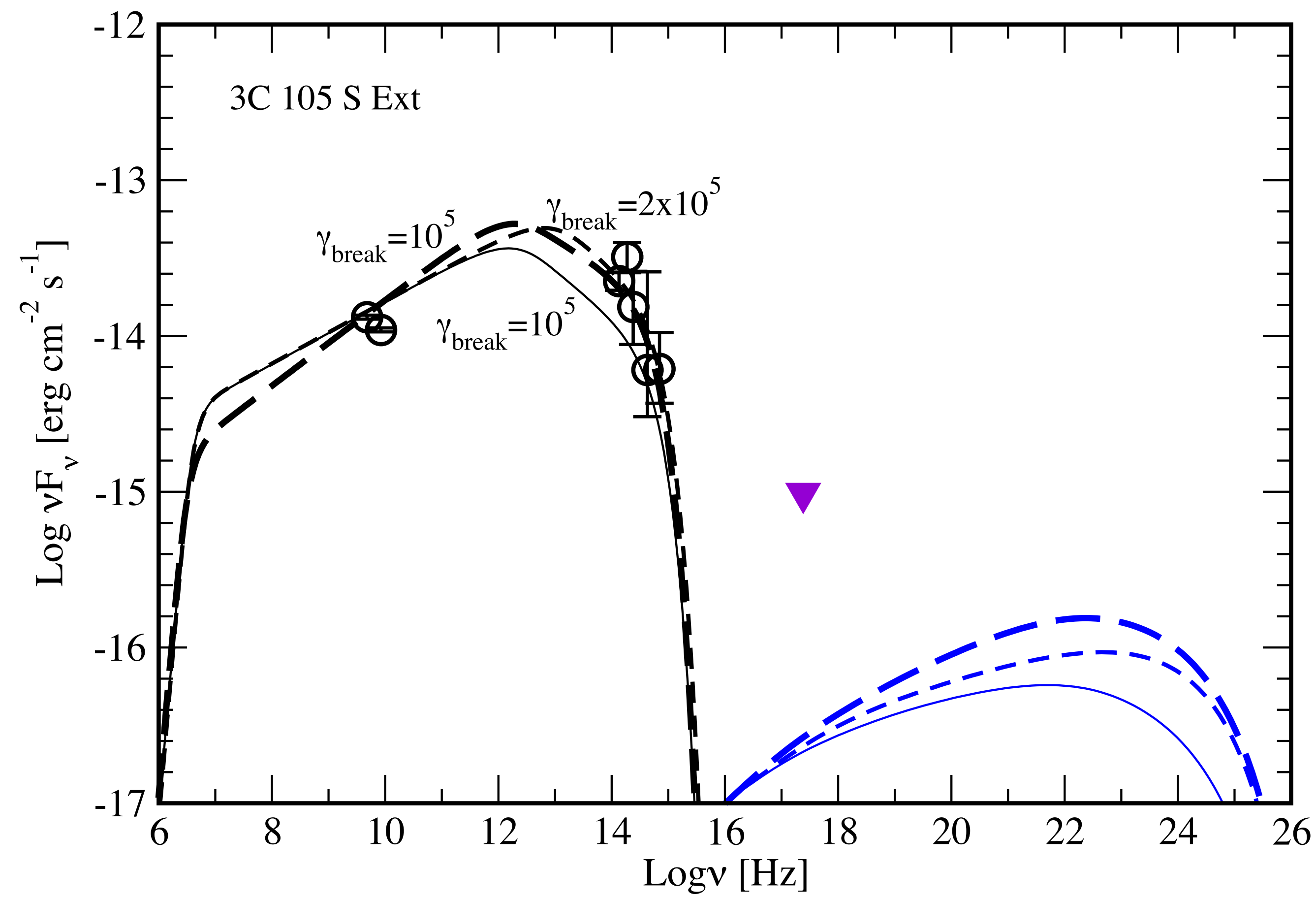

- The radio to NIR-optical SED can be modeled assuming a single power law EED and energy equipartition between magnetic field and particles;
- test 1: the non-detection in X-rays sets a lower limit to the magnetic field Bmin>7 μG;
- test 2: lower limit to a possible break is $\gamma_{break,\ ext} \geq 10^5$.

$\gamma_{max,\ ext} \sim 8\times10^5$ => $t_{rad} \sim 10^{3\text{-}4}$ yrs
$L_{ext,proj} \sim 4$ kpc

consistent with particles diffusing out of the main front shock region?

Diffusion vs re-acceleration

Free streaming along (ordered) magnetic field lines implies:

i) particles are not accelerated once they left the front shock $\gamma_{break,\ ext} \leq \gamma_{break,comp}$;

ii) diffusion time must be shorter than the synchrotron cooling time $\tau_{diff} \leq \tau_{syn}$;

+ (loose constrain) on the non detection in X-rays: $B \geq B_{min,IC}$

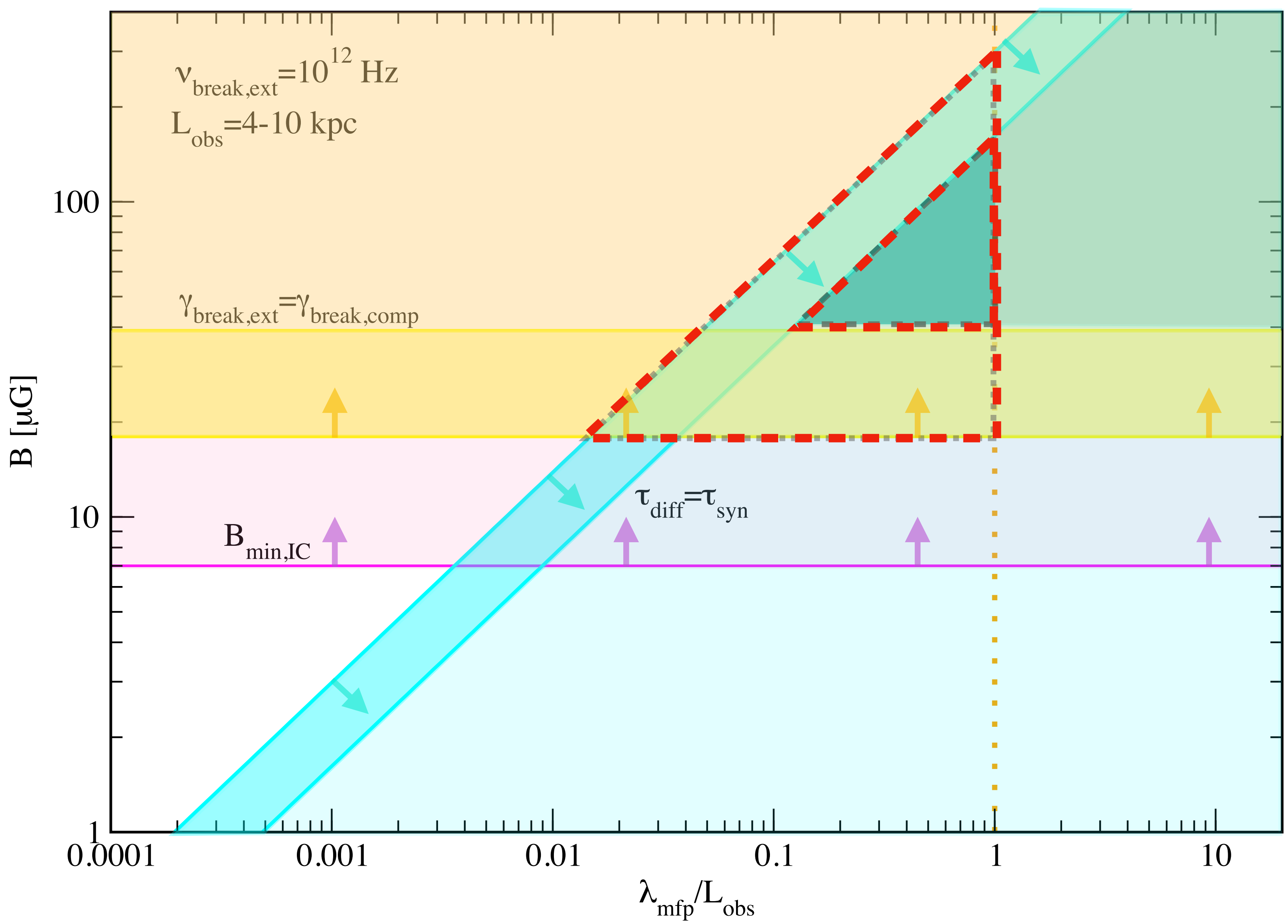

Diffusion scenario restricted to a narrow B vs λ range

efficient acceleration mechanism in the post-shock region able to re-energize particles up to $\gamma \sim 10^6$?

i) $\gamma_{break,\,ext} \leq \gamma_{break,comp}$

$B \geq (2.38e\text{-}7 \times \nu_{break,ext.obs})^{1/2} / (\gamma_{break,comp})^2$

$\gamma_{break,comp}$ from the modeling of the compact regions;

ii) $\tau_{diff} \leq \tau_{syn}$

$\tau_{diff} = 3/4 \times L_{obs}^2 / \lambda_{mfp}$

$\tau_{syn} = 1.59e12 \times B^{-3/2} / (\nu \times (1+z))^{1/2}$

$B_{\mu G} \leq 7.5e3 \times 1/(\nu_{GHz} \times (1+z))^{1/3} \times 1/(L_{obs,kpc})^{2/3} \times (\lambda_{mfp,kpc}/L_{obs,kpc})^{2/3}$

iii) $B \geq B_{min,IC}$

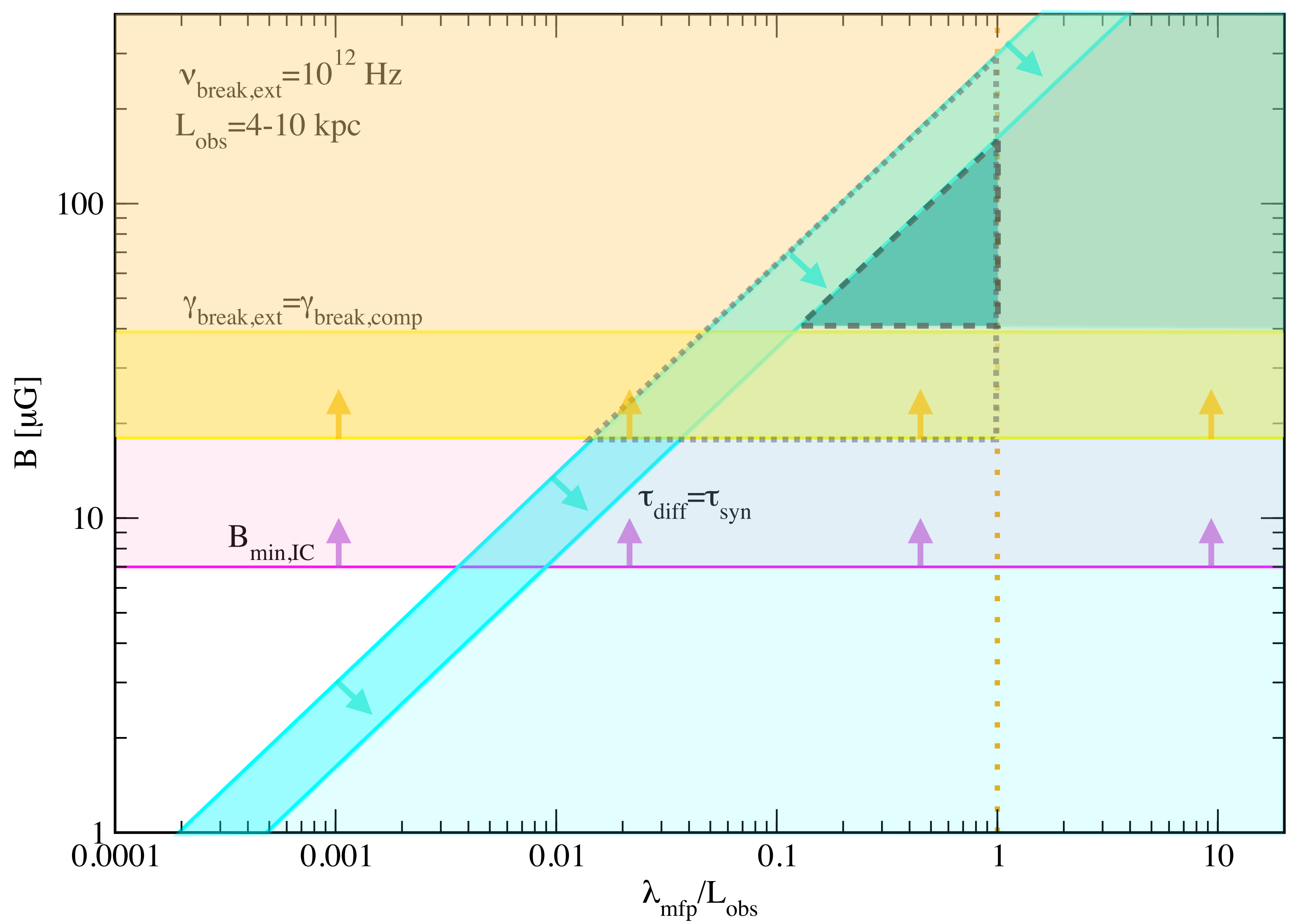

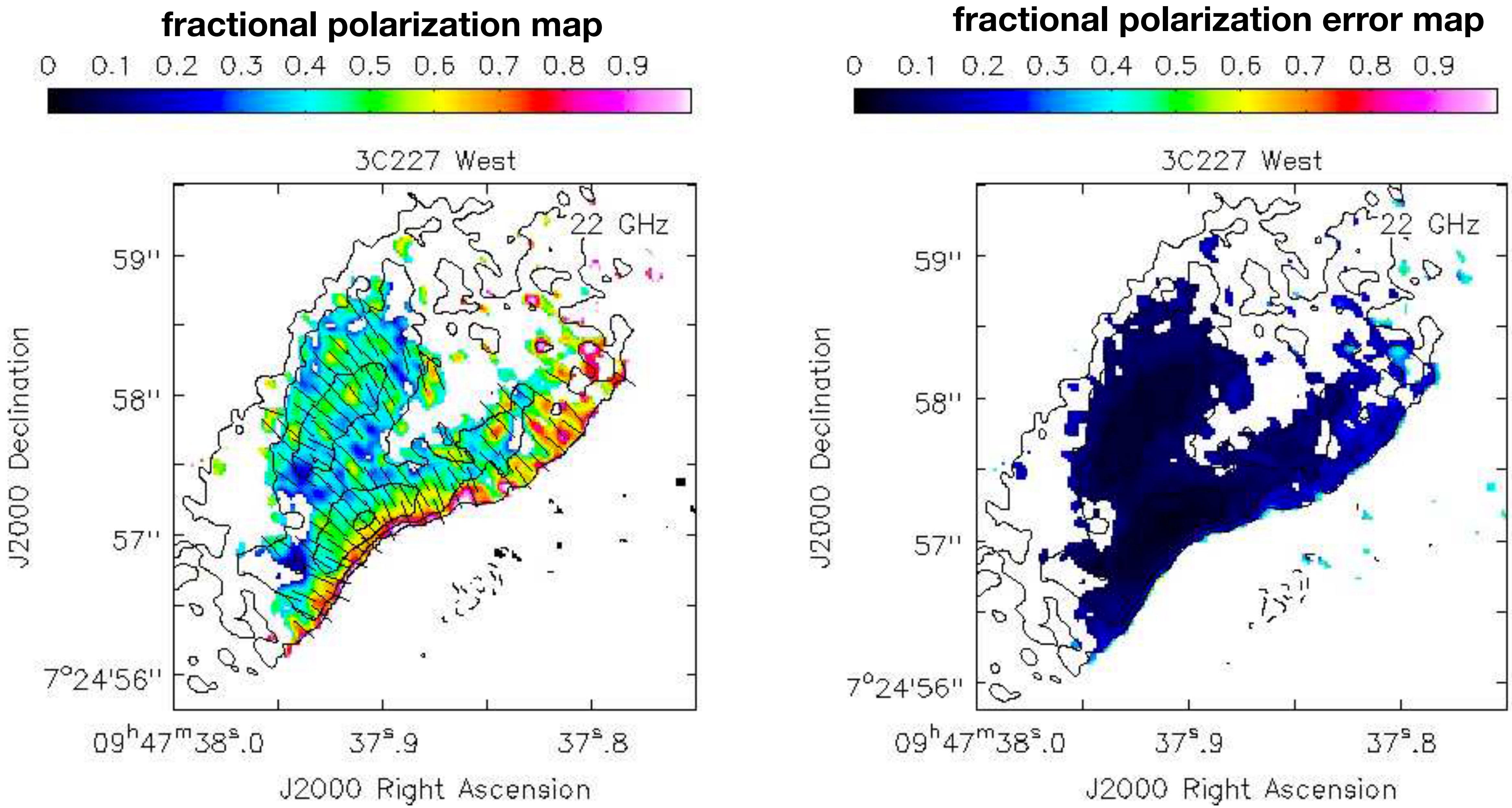

Figure 3. VLA images at 22 GHz of the hotspot 3C 227 West. *Left panel*: Fractional polarization image; *right panel*: fractional polarization error image. Contours represent the total intensity with natural weighting. The first contour is 21 μJy beam^{-1} and corresponds to three times the off-source noise level measured on the image plane. Contours increase by a factor of 2. The colour scale is shown by the wedge at the top of each image. Vectors represent the electric vector position angle. The restoring beam is plotted on the bottom left corner of each image.

- polarization reaches values up to 70 per cent=> highly ordered magnetic field with size up to a hundred parsecs;
- on average the polarization of the hotspot component is about 30– 50 per cent=> presence of a significant random field component;
- the polarization vectors are perpendicular to the source structure => a magnetic field parallel to the shock direction;
- displacement between the peaks in polarized intensity and in total intensity images=> on small scales both an ordered and a turbulent magnetic field component co-exist?

Name	4.8 GHz (mJy)	8.4 GHz (mJy)	K (μJy)	H (μJy)	J (μJy)	R (μJy)	B (μJy)
3C 105 S1	26.4±0.7	18.4±0.5	2.59±0.16	2.80±0.24	$1.12^{+0.23}_{-0.24}$	$0.29^{+0.35}_{-0.16}$	<0.10
3C 105 S2	539.7±16.2	371.8±11.1	14.43±0.39	$13.54^{+0.66}_{-0.63}$	$5.76^{+1.03}_{-0.86}$	$1.03^{+1.24}_{-0.53}$	$0.21^{+0.08}_{-0.06}$
3C 105 S3	402.9±12.1	259.6±7.8	$23.35^{+0.54}_{-0.52}$	$22.68^{+0.95}_{-0.92}$	$8.48^{+1.48}_{-1.27}$	$1.30^{+1.56}_{-0.70}$	$0.30^{+0.10}_{-0.06}$
3C 105 S Ext	275.2±8.2	130.3±3.9	16.65±2.32	$17.16^{+2.31}_{-2.22}$	$6.38^{+3.80}_{-3.24}$	$1.41^{+4.85}_{-1.41}$	$0.88^{+0.47}_{-0.35}$
3C 195 S	-	94.0±2.8	$3.25^{+0.82}_{-0.73}$	<0.46	-	$0.26^{+0.01}_{-0.02}$	$0.14^{+0.01}_{-0.01}$
3C 227 E1	102.4±3.1	-	<1.10	-	-	$0.19^{+0.07}_{-0.06}$	<0.14
3C 227 E2	83.9±2.5	-	<1.10	-	-	$0.35^{+0.11}_{-0.09}$	$0.53^{+0.16}_{-0.13}$
3C 227 W1	90.4±2.7	63.1±1.9	$10.74^{+1.51}_{-1.44}$	$9.51^{+0.60}_{-1.30}$	$5.27^{+0.66}_{-0.61}$	1.19±0.11	$1.02^{+0.23}_{-0.20}$
3C 227 W2	28.3±0.8	15.7±0.5	$9.53^{+1.32}_{-1.26}$	$4.29^{+0.86}_{-0.77}$	$2.88^{+0.44}_{-0.40}$	$0.44^{+0.07}_{-0.06}$	$0.41^{+0.11}_{-0.09}$

	R kpc	B μG	$\gamma_{min}/\gamma_{max}/\gamma_{break}$	p_1/p_2	Γ_{bulk}	θ deg.	(U_B/U_e)
					3C 105 S Ext		
Model 1	4.9	42	100/8e5/–	2.6/–	1.0	45	1.0
Model 2	4.9	7	100/2e6/–	2.6/–	1.0	45	0.0013
					3C 195 S		
Model 1	2.8	76	100/1.e6/–	3.05/–	1.0	45	1.0
Model 2	2.8	10	100/2.0e6/–	3.05/–	1.0	45	2.1e-3
Model 3	1.0	14.5	100/1.7e6/3.e3	2.05/3.05	1.0	45	2.3e-4
Model 4	1.0	53	100/7e5/–	3.05/–	3.0	18.0	1.0
					3C 227 W1		
Model 1	1.6	72	100/9e5/–	2.6/–	1.0	45.0	1.0
Model 2	1.6	2.1	100/5e6/1.5e6	2.4/3.4	1.0	45.0	3.1e-6
Model 3	1.6	13	100/1.5e6/2e5	2.4/3.4	4.0	18.0	0.15